SUPPORTING INFORMATION

Time Evolution of the Wettability of Supported Graphene Under Ambient Air Exposure

Adrianus I. Aria,[†] Piran R. Kidambi,[†§] Robert S. Weatherup,[†‖] Long Xiao,[†] John A. Williams,[‡] and Stephan Hofmann[*†]

[†] Division of Electrical Engineering, and [‡]Division of Mechanics, Materials and Design, Department of Engineering, University of Cambridge, United Kingdom CB2 1PZ

[§] Department of Mechanical Engineering, Massachusetts Institute of Technology, Cambridge, MA, United States 02139-4307

[‖] Materials Sciences Division, Lawrence Berkeley National Laboratory, Berkeley, CA, United States 94720

* Corresponding Author: sh315@cam.ac.uk

1. Effect of surface inhomogeneity

It has been known that surface inhomogeneity, either chemical or topographical, strongly influence the apparent wettability of a sample.[1] Although it is a not entirely correct, it can be assumed that as grown CVD graphene samples tested in this current study are chemically homogeneous. This assumption is based on the fact that during the contact angle measurements, no liquid droplets were observed to be strongly confined to or repelled from any particular area of the surface of graphene samples.[2] On the other hand, the topographical inhomogeneity, or widely known as surface roughness, of supported graphene can be measured and included in the wettability measurement. Thus, in this current study, the graphene wettability is presented in terms of Young's CA, which can be obtained from the apparent CA by the following relation:

$$\cos\theta_A = AR\cos\theta_Y \quad (1)$$

With θ_A is the apparent CA, θ_Y is the Young's CA, and AR is the area ratio. AR is defined as a ratio between the apparent area and the projected area, which is a measure of surface roughness. Equation 1 shows that the effect of AR to the difference between Young's CA and apparent CA is more significant for low apparent CA values. For hydrophobic graphene samples, with apparent CA values closer to 90°, the effect of topographical inhomogeneity to graphene wettability is negligible. On the other hand, for relatively hydrophilic graphene samples, the effect of topographical inhomogeneity on graphene wettability is more significant.

Here, AR is obtained from atomic force microscopy (AFM) measurements that were performed in air at ambient pressure and temperature (Digital Instruments, Dimension 3100). Surface topography was acquired in a tapping mode at a frequency of 1Hz, a resolution of 2048x1024 pixels, and a scan size of 20x20 μm^2 or 25x25 μm^2. From AFM measurements, it is found that the maximum value of AR for supported graphene and bare metal reference substrates

is about 1.085, which is close to unity (Figure S 1 and Figure S 2). Our data show that the largest differences between Young's CA and apparent CA are found mostly on samples that have only been exposed to ambient air for less than 1 week, and are similar in magnitude with the measurement uncertainty, which is about ±3°. For samples that have been exposed to ambient air for months, the differences between Young's CA and apparent CA are negligible. Based on this, it is reasonable to consider that the effect of topographical inhomogeneity on the time evolution of graphene wettability is minimal. Nevertheless, in this current study, all wettability measurements are represented by Young's CA.

2. Wetting transparency hypotheses

A. Non-wetting transparency

The plot of WCA graphene/substrate vs WCA HOPG (Figure 2b) shows the correlation between WCA of supported graphene and that of HOPG at each corresponding ambient air exposure time point, for the purpose of testing the hypothesis of whether or not supported graphene is non-wetting transparent. According to this hypothesis, graphene is considered non-wetting transparent if its WCA is equal to that of bulk graphite (HOPG).[3] A simple linear regression, with WCA of supported graphene as the dependent variables and WCA of HOPG as the regressors, is used to test this hypothesis. For supported graphene on Cu substrate (G/Cu), the simple linear regression is modeled as following:

$$\mathrm{WCA\_G/Cu} = \beta_{GCu}\,\mathrm{WCA\_HOPG} + \alpha_{GCu} \qquad (2)$$

with β_{GCu} is the slope of linear regression and α_{GCu} is the intercept. Using ordinary least-square estimator, the fitted values of β_{GCu} and α_{GCu} are summarized in Table S 1. Similarly, for supported graphene on Ni substrate (G/Ni), the simple linear regression is modeled as following:

$$WCA\_G/Ni = \beta_{GNi}\, WCA\_HOPG + \alpha_{GNi} \quad (3)$$

with β_{GNi} is the slope of linear regression and α_{GNi} is the intercept. Using ordinary least-square estimator, the fitted values of β_{GNi} and α_{GNi} are summarized in Table S 2.

As shown in Table S 1, α_{GCu} has an estimated value of -3.894 at a p value of 0.596. Since the p value of α_{GCu} is much larger than the 5% significance level threshold, it can be assumed that α_{GCu} has a real value that is not significantly different from zero. This implies that WCA of G/Cu is statistically the same as WCA of HOPG if the ambient air exposure time is set to zero. Furthermore, β_{GCu} has an estimated value of 1.018 at a p value of 6.262×10^{-12}, which is much smaller than the 5% significance level threshold. The fact that the regression slope is significantly close to unity implies that WCA of G/Cu is statistically the same as WCA of HOPG at all observed ambient air exposure time points. Therefore, the hypothesis of non-wetting transparency of G/Cu, where WCA of G/Cu is equal to that of HOPG, is statistically accepted at 95% confidence level within 1 year of ambient air exposure.

In contrast, as shown in Table S 2, α_{GNi} has an estimated value of 58.282 at a p value of 2.391×10^{-12}, which is much smaller than the 5% significance level threshold. The nonzero value of α_{GNi} implies that WCA of G/Ni is statistically different from that of HOPG if the ambient air exposure time is set to zero. Furthermore, β_{GNi} has an estimated value of 0.416 at a p value of 7.601×10^{-08}, which is also much smaller than the 5% significance level threshold. This implies that the time dependent changes in WCA of G/Ni is significantly different than that of HOPG. While WCA of G/Ni is linearly correlated to WCA of HOPG, their relationship does not necessarily mean causation and is rather meaningless. Therefore, the hypothesis of non-wetting transparency of G/Ni, where WCA of G/Ni is equal to that of HOPG, cannot be statistically accepted at 95% confidence level within 1 year of ambient air exposure.

B. Complete wetting transparency

The plot of WCA graphene/substrate vs WCA substrate (Figure 2c) shows the correlation between WCA of supported graphene and that of bare metal substrate at each corresponding ambient air exposure time point, for the purpose of testing the hypothesis of whether or not supported graphene is completely wetting transparent. According to this hypothesis, graphene is considered wetting transparent if its WCA is equal to that of bare metal substrate.[4] A simple linear regression, with WCA of supported graphene as the dependent variables and WCA of bare metal substrate as the regressors, is used to test this hypothesis. For supported graphene on Cu substrate (G/Cu), the simple linear regression is modeled as following:

$$WCA\_G/Cu = \beta_{GCu}\, WCA\_Cu + \alpha_{GCu} \quad (4)$$

with β_{GCu} is the slope of linear regression and α_{GCu} is the intercept. Using ordinary least-square estimator, the fitted values of β_{GCu} and α_{GCu} are summarized in Table S 3. Similarly, for supported graphene on Ni substrate (G/Ni), the simple linear regression is modeled as following:

$$WCA\_G/Ni = \beta_{GNi}\, WCA\_Ni + \alpha_{GNi} \quad (5)$$

with β_{GNi} is the slope of linear regression and α_{GNi} is the intercept. Using ordinary least-square estimator, the fitted values of β_{GNi} and α_{GNi} are summarized in Table S 4.

As shown in Table S 3, α_{GCu} has an estimated value of 47.944 at a p value of 1.967×10^{-18} and β_{GCu} has an estimated value of 0.468 at a p value of 4.748×10^{-15}. The fact that both values satisfy the 5% significance level threshold implies that the time dependent changes in WCA of G/Cu is not statistically the same as that of bare Cu substrate at all observed and zero ambient air exposure time points. Similarly, as shown in Table S 4, α_{GNi} has an estimated value of 75.236 at a p value of 5.221×10^{-24} and β_{GNi} has an estimated value of 0.226 at a p value of 1.759×10^{-09}.

The fact that both values satisfy the 5% significance level threshold implies that the time dependent changes in WCA of G/Ni is significantly different than, and almost independent of, that of bare Ni substrate at all observed and zero ambient air exposure time points. Although there is a weak linear relationship between WCA of G/Cu and WCA of bare Cu substrate, and an even weaker linear relationship between WCA of G/Ni and WCA of bare Ni substrate, both relationship do not necessarily mean causation and may not have any physical interpretations. Therefore, both the hypothesis of complete wetting transparency of G/Cu, where WCA of G/Cu is equal to that of bare Cu substrate, and that of G/Ni, where WCA of G/Ni is equal to that of bare Ni substrate, cannot be statistically accepted at 95% confidence level within 1 year of ambient air exposure.

It can be easily speculated that the complete wetting transparency argument may arise from the fact that for t > 6 months, WCA of graphene is highly comparable to that of bare metal substrate. In other words, the wettability of contaminant saturated graphene is the same as that of contaminant saturated bare metal substrate. While this is expected, it does not bear any significance as the WCA values being compared are from the accumulated contaminants and not from the graphene and metal substrate themselves. Therefore, this comparison should not be used to draw any conclusions about wetting transparency. Instead, it should be used as evidence that WCA is dictated by contaminants accumulation and the WCA values for different materials tends to be the same once their surfaces have been saturated by the contaminants.

3. Water-graphene interaction potential

Based on the measured CA, the interaction potential per unit area (-Φ) between water and graphene could be estimated using the modified Young-Dupré equation as following: $\gamma_L(1 +$

$\cos\theta) = -\phi$, where γ_L is the surface tension of water (72.8 mJ m^{-2}).[5] Expectedly, the calculated -Φ decreases monotonically with the increase of ambient air exposure time (Figure S 3). Within 1 hour of ambient air exposure, -Φ of HOPG and G/Cu is calculated at about 97.9 and 100.3 mJ m^{-2} respectively, which is in a good agreement with that previously reported.[6] For G/Ni at the same ambient air exposure time, -Φ is found to be significantly lower at about 79.6 mJ m^{-2}. The high initial value of –Φ, which is higher than the surface tension of water, confirms that graphene is initially hydrophilic. Since -Φ does not decrease further beyond the value of 66-69 mJ m^{-2}, we consider this as the equilibrium –Φ, which was previously calculated as the -Φ of suspended monolayer graphene without taking into account the contamination adsorption effect.[7]

4. Determination of surface free energy

The surface free energy of graphene can be calculated using various methods that hinge on contact angle measurements. The measured contact angles are then fitted into a specific surface energy model to determine the surface free energy. The magnitude and interpretation of the calculated surface free energy may vary depending on the model used. Thus, in this study, we only employ models that have been commonly used and widely accepted. Typically several test liquids with different surface energy components are used for measurement. The test liquids used in the measurement have to be pure compounds, not mixtures, to avoid selective surface adsorption.[8] Furthermore, the surface energy of these test liquids has to be greater than that of the graphene samples. To satisfy these conditions, eight test liquids were initially used in this study, including heptane, paraffin, bromonaphtalene, diiodomethane, ethylene glycol, formamide, glycerol, and water. The contact angle of these liquids on graphene samples were then measured and tested against the Zisman critical surface energy criteria to determine their suitability.[9]

Subsequently, four models, including the Owens-Wendt (OW) model,[10] the van Oss-Chaudhury-Good (OCG) model,[11] the adjusted van Oss-Chaudhury-Good (aOCG) model,[12] and the Chang-Chen (CC) model,[13,14] were used to determine the surface free energy of supported graphene, along with graphite (HOPG) and bare metal (graphene free) substrates, from contact angle data. The Fowkes model is not included in this study due to its similarity to the OW model. The Neumann model is also not included in this study as it has been proven that using only one fitting parameter is insufficient to reliably calculate surface energy.[8,10] Details of the methods are described below and the results are summarized in Figure S 14.

A. Zisman critical surface energy model

The Zisman model is basically an empirical model that shows the linear relation between surface energy (γ_L) and contact angle (θ) of homologous liquids according to the following relation:

$$\cos\theta = 1 + \beta(\gamma_C - \gamma_L) \quad (6)$$

where γ_C is the Zisman critical surface energy of the solid sample and β is a fitting constant. Table S 1 shows a list of test liquids and their γ_L that are used herein to determine γ_C.[9] Linear regression of the experimental data allows for determination of β as the regression slope and γ_C at which $\cos\theta = 1$. Here, ordinary least square method is used as the estimator. While the Zisman model lacks of theoretical rigor for determination of surface energy,[8] the obtained γ_C could still be used to determine the suitability of the test liquids. Since liquids with $\gamma_L < \gamma_C$ wet the surface completely, only liquids with $\gamma_L < \gamma_C$ that are used for the determination of surface free energy of graphene. Figure S 8 shows that for supported graphene that has been exposed to 1 hour of ambient air, γ_C = 41-42 mJ/m^2. On the other hand, for supported graphene that has been

exposed to 1 year of ambient air, γ_C = 37-38 mJ/m^2. While the obtained γ_C is not the actual surface free energy of supported graphene, this finding suggests that the surface free energy of supported graphene decreases with the increase of ambient air exposure time. This finding also implies that heptane and paraffin, both have γ_L that are much smaller than γ_C of graphene, cannot be used in the determination of surface free energy of graphene.

B. Owens-Wendt (extended Fowkes) surface energy model

The Owens-Wendt (OW) model describes the relation between surface energy (γ_L) of liquids in terms of its dispersive (γ_L^D) and polar (γ_L^P) components, as well as their contact angle (θ), according to the following relation:

$$\gamma_L(1+\cos\theta) = 2\,(\gamma_L^D\gamma_S^D)^{\frac{1}{2}} + 2\,(\gamma_L^P\gamma_S^P)^{\frac{1}{2}} \quad (7)$$

where γ_S^D and γ_S^P are the dispersive and polar components of the surface free energy (γ_S) of the solid sample, which is given by the following relation:

$$\gamma_S = \gamma_S^D + \gamma_S^P \quad (8)$$

Table S 1 shows a list of test liquids with their γ_L as well as their γ_L^D and γ_L^P components used for determining γ_S. Two variables linear regression of the experimental data with zero intercept allows for direct determination of γ_S^D as the square of the first regression slope and γ_S^P as the square of the second one. Here, ordinary least square method is used as the estimator. Figure S 9 shows that within 1 hour of ambient air exposure, γ_S^D of G/Cu, G/Ni, and HOPG is measured around 40-42 mJ/m^2, which then decreases to 37-39 mJ/m^2 after 1 year of ambient air exposure. While γ_S^D is similar for all supported graphene and graphite samples, the variation in γ_S^D between different samples is rather large. Figure S 9 shows that within 1 hour of ambient air exposure, γ_S^P

of G/Cu and HOPG is measured around 5-7 mJ/m^2, which then decreases to 0.2-0.6 mJ/m^2 after 1 year of ambient air exposure. On the other hand, within 1 hour of ambient air exposure, γ_S^P of G/Ni is measured around 1 mJ/m^2, which then decreases to 0.1 mJ/m^2 after 1 year of ambient air exposure. Here we found that the γ_S of 1 hour old G/Cu and HOPG is indeed comparable to that reported in literatures.[15] Despite of this similarity, we exclude this finding in our main report due to the obsolescence of the OW model.[8] Here, the fitting of experimental data using the OW model is only for comparison purpose. It has to be noted that the polar component (γ^P) of this model only refers to dipole-dipole (Debye) interactions, which is inadequate to describe the acid-base interactions and especially the monopolarity and dipolarity phenomena.[8]

C. van Oss-Chaudhury-Good surface energy model

The van Oss-Chaudhury-Good (OCG) model describes the relation between surface energy (γ_L) of liquids in terms of its Lifshitz-van der Waals (γ_L^{LW}) and Lewis acid-base (γ_L^{AB}) components, as well as their contact angle (θ), according to the following relation:

$$\gamma_L(1+\cos\theta) = 2\,(\gamma_L^{LW}\gamma_S^{LW})^{\frac{1}{2}} + 2\,(\gamma_L^{+}\gamma_S^{-})^{\frac{1}{2}} + 2\,(\gamma_L^{-}\gamma_S^{+})^{\frac{1}{2}} \quad (9)$$

where γ_L^+ and γ_L^- are the Lewis acid and Lewis base parameters of the liquids respectively, and γ_S^+ and γ_S^- are the Lewis acid and Lewis base parameters of the solid respectively. The Lewis acid-base component is then estimated using the geometric mean rule as follows:

$$\gamma_i^{AB} = 2\,(\gamma_i^{+}\gamma_i^{-})^{\frac{1}{2}} \quad (10)$$

and the total surface free energy (γ_S) of the solid sample is given by the following relation:

$$\gamma_S = \gamma_S^{LW} + \gamma_S^{AB} \quad (11)$$

Table S 2 shows a list of test liquids with their γ_L as well as their γ_L^{LW} and γ_L^{AB} components used for determining γ_S. In order to perform two variables linear regression of the experimental data, equation (9) is rearranged as following:

$$\frac{\gamma_L(1+\cos\theta)}{2\,(\gamma_L^{LW})^{\frac{1}{2}}} = (\gamma_S^-)^{\frac{1}{2}}\left(\frac{\gamma_L^+}{\gamma_L^{LW}}\right)^{\frac{1}{2}} + (\gamma_S^+)^{\frac{1}{2}}\left(\frac{\gamma_L^-}{\gamma_L^{LW}}\right)^{\frac{1}{2}} + (\gamma_S^{LW})^{\frac{1}{2}} \quad (12)$$

The first regression slope is the square root of γ_S^-, while the second regression slope is the square root of γ_S^+. The γ_S^{LW} is determined from the square of the zero intercept. Here, ordinary least square method is used as the estimator. Figure S 10 shows the fitting of experimental data and the obtained values of γ_S^{LW}, γ_S^+, and γ_S^- for supported graphene, along with graphite (HOPG) and bare metal (graphene free) substrates, within 1 hour and 1 year of ambient air exposure. It has to be noted that unlike in the OW model, the Lifshitz-van der Waal component of the OCG model takes into account all non-bonding orbital interactions, including Keesom (dipole-dipole), Debye (dipole-induced dipole) and London (induced dipole-induced dipole) interactions, while its Lewis acid-base component includes electron donation and acceptance bonding.[11]

D. Adjusted van Oss-Chaudhury-Good surface energy model

The adjusted van Oss-Chaudhury-Good (aOCG) model is essentially the OCG model, which is modeled as equation (9), but with adjusted fitting parameters.[12] In the OCG model, water is presumably a perfectly balanced amphoteric compound with the same acidic and basic strengths. In contrast, the aOCG model presumes that water is more electrophilic than it is nucleophilic, such that it bonds to other molecules by accepting electrons rather than donating ones. Table S 3 shows the adjusted parameters for test liquids used in the aOCG model with their γ_L as well as their γ_L^{LW} and γ_L^{AB} components. Figure S 11 shows the fitting of experimental data and the

obtained values of γ_S^{LW}, γ_S^+, and γ_S^- for supported graphene, along with graphite (HOPG) and bare metal (graphene free) substrates, within 1 hour and 1 year of ambient air exposure.

E. Chang-Chen surface energy model

The Chang-Chen (CC) model describes the relation between surface energy (γ_L) of liquids in terms of its Lifshitz-van der Waals (γ_L^{LW}) and Lewis acid-base (γ_L^{AB}) components, as well as their contact angle (θ), according to the following relation:

$$\gamma_L(1+\cos\theta) = P_L^{LW}P_S^{LW} - \left(P_L^a P_S^b + P_L^b P_S^a\right) \quad (13)$$

where P_L^a and P are the Lewis acid and Lewis base parameters of the liquids respectively, and P_S^a and P_S^b are the Lewis acid and Lewis base parameters of the solid sample respectively. The Lewis acid-base component is then estimated using the following relation:

$$\gamma_i^{AB} = -P_i^a P_i^b \quad (14)$$

and the Lifshitz-van der Waals component is then estimated using the following relation:

$$\gamma_i^{LW} = \frac{1}{2}(P_i^{LW})^2 \quad (15)$$

Combining equation (14) and (15), the total surface free energy (γ_S) of the solid sample is given by the following relation:

$$\gamma_S = \gamma_S^{LW} + \gamma_S^{AB} = \frac{1}{2}(P_S^{LW})^2 - P_S^a P_S^b \quad (16)$$

Table S 4 shows a list of test liquids with their γ_L as well as their P_L^{LW}, P_L^a, and P_L^b components used for determining γ_S. In order to perform two variables linear regression of the experimental data, equation (13) is rearranged as following:

$$\frac{\gamma_L(1+\cos\theta)}{P_L^{LW}} = -P_S^b\frac{P_L^a}{P_L^{LW}} - P_S^a\frac{P_L^b}{P_L^{LW}} + P_S^{LW} \quad (17)$$

The first regression slope is the negative of P_S^b, while the second regression slope is the negative of P_S^a. The P_S^{LW} is determined from the square of the zero intercept. Here, ordinary least square method is used as the estimator. Figure S 12 shows the fitting of experimental data and the obtained values of P_S^{LW}, P_S^a, and P_S^b for supported graphene, along with graphite (HOPG) and bare metal (graphene free) substrates, within 1 hour and 1 year of ambient air exposure. Unlike the OCG model, the CC model allows for both attractive and repulsive interactions. Furthermore, the CC model presumes that water is more nucleophilic than it is electrophilic, such that it bonds to other molecules by donating electrons rather than accepting ones.[13,14]

Tables

Table S 1. Fitted regression parameters for WCA of G/Cu vs WCA of HOPG

Predictor	Estimate value	Std. Error	t value	p value
αGCu	-3.894	7.257	-0.536	0.596
βGCu	1.018	0.086	11.784	6.262 x 10-12
Root MSE	4.71			
R-sq	0.842	Adj. R-sq	0.836	

Table S 2. Fitted regression parameters for WCA of G/Ni vs WCA of HOPG

Predictor	Estimate value	Std. Error	t value	p value
α_{GNi}	58.282	4.736	12.307	2.391×10^{-12}
β_{GNi}	0.416	0.056	7.388	7.601×10^{-08}
Root MSE	3.07			
R-sq	0.677	Adj. R-sq	0.665	

Table S 3. Fitted regression parameters for WCA of G/Cu vs WCA of Cu

Predictor	Estimate value	Std. Error	t value	p value
α_{GCu}	47.944	2.158	22.212	1.968×10^{-18}
β_{GCu}	0.468	0.029	16.116	4.749×10^{-15}
Root MSE	3.57			
R-sq	0.909	Adj. R-sq	0.906	

Table S 4. Fitted regression parameters for WCA of G/Ni vs WCA of Ni

Predictor	Estimate value	Std. Error	t value	p value
α_{GNi}	75.236	2.035	36.972	5.221×10^{-24}
β_{GNi}	0.226	0.025	9.014	1.759×10^{-09}
Root MSE	2.66			
R-sq	0.758	Adj. R-sq	0.748	

Table S 5. Surface energy and its components of the test liquids for Zisman model and Owens-Wendt model.[910]

Liquid	γ_L	γ_L^D	γ_L^P
Heptane	20.14	20.14	0
Paraffin	26	26	0
Bromonaphtalene	44.4	44.4	0
Diiodomethane	50.8	50.8	0
Ethylene Glycol	48	29	19
Formamide	58	39	19
Glycerol	64	34	30
Water	72.8	21.8	51

Table S 6. Surface energy and its components of the test liquids according to van Oss–Chaudhury–Good model.[11]

Liquid	γ_L	γ_L^{LW}	γ_L^{AB}	γ_L^{+}	γ_L^{-}
Heptane	20.14	20.14	0	0	0
Paraffin	26	26	0	0	0
Bromonaphtalene	44.4	44.4	0	0	0
Diiodomethane	50.8	50.8	0	0	0
Ethylene Glycol	48	29	19	1.92	47
Formamide	58	39	19	2.28	39.6
Glycerol	64	34	30	3.92	57.4
Water	72.8	21.8	51	25.5	25.5

Table S 7. Surface energy and its components of the test liquids according to adjusted van Oss–Chaudhury–Good model.[12]

Liquid	γ_L	γ_L^{LW}	γ_L^{AB}	γ_L^{+}	γ_L^{-}
Heptane	20.14	20.14	0	0	0
Paraffin	26	26	0	0	0
Bromonaphtalene	44.4	44.4	0	0	0
Diiodomethane	50.8	50.8	0	0	0
Ethylene Glycol	47.8	31.4	16.4	1.58	42.5
Formamide	58.2	35.6	22.6	1.95	65.7
Glycerol	63.9	34.4	29.5	16.9	12.9
Water	72.8	21.8	51	65	10

Table S 8. Surface energy and its components of the test liquids according to Chang-Chen model. [13,14]

Liquid	γ_L	γ_L^{LW}	P_L^{LW}	P_L^a	P_L^b
Heptane	23.8	23.8	6.9	0	0
Paraffin	26	26	7.21	0	0
Bromonaphtalene	44.93	55.125	10.5	-2.67	-3.82
Diiodomethane	50.35	67.28	11.6	-4.11	-4.12
Ethylene Glycol	48.2	28.125	7.5	3.69	-5.44
Formamide	58.75	26.645	7.3	6.92	-4.64
Glycerol	63.62	32	8	3.4	-9.3
Water	72.69	21.78	6.6	6.88	-7.4

Figures

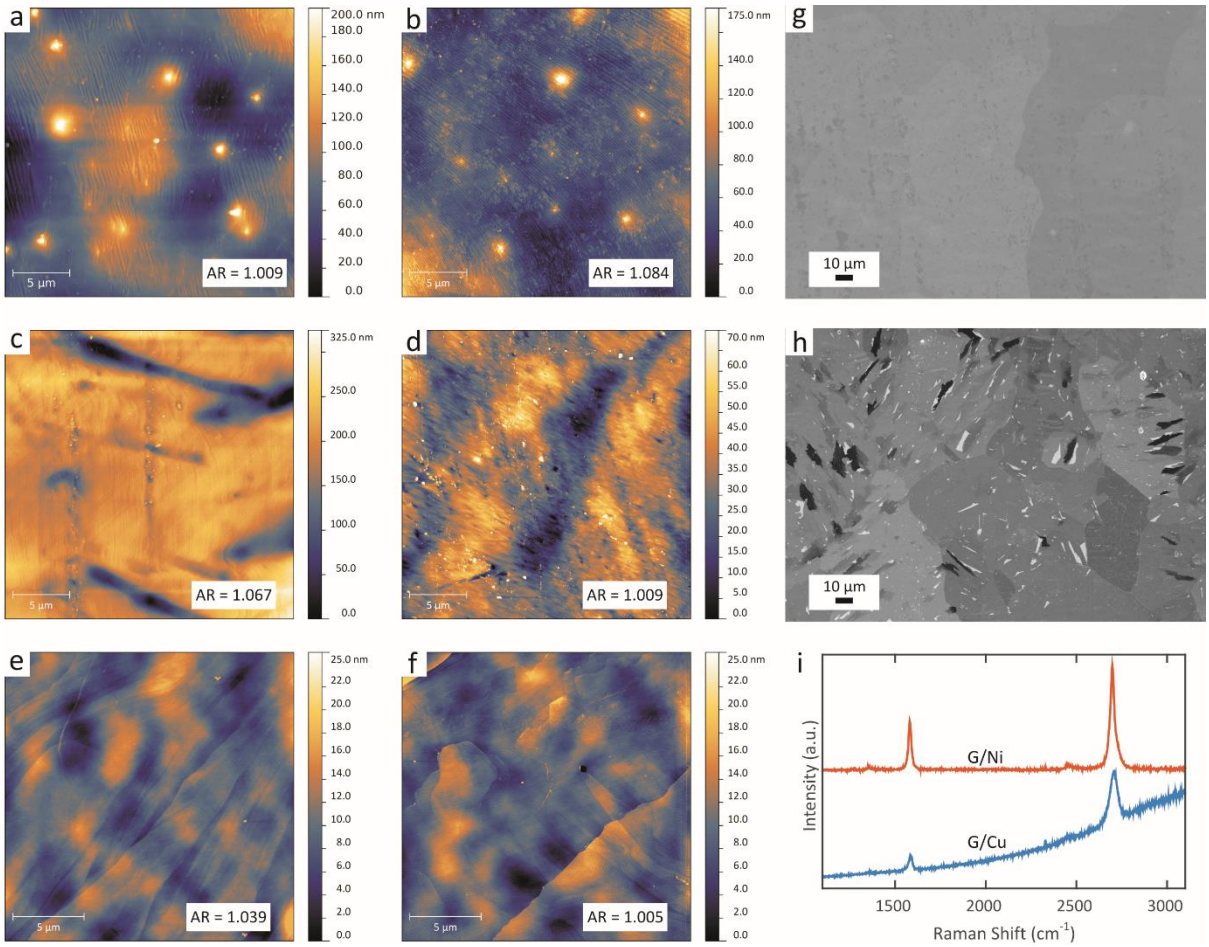

Figure S 1. AFM images of G/Cu (a, b), G/Ni (c, d), and HOPG (e, f) taken at different ambient air exposure time points. The images in (a, c) and (e) are taken from samples with t = ~1 week and t = ~1 hour, respectively, while those in (b, d, and f) are taken from samples with t = ~1 year. AR is the area ratio that is defined as the ratio between the apparent area and the projected area obtained from AFM measurement. Since AR is close to unity for all samples, the effect of topographical inhomogeneity to the graphene wettability can be considered as minimal. Nevertheless, in this study, all wettability measurements are represented by Young's CA that takes into account topographical inhomogeneities. Low magnification SEM images of G/Cu (g) and G/Ni (h) showing the predominantly mono-layer graphene with almost a complete coverage

of the growth substrates by the graphene layer. Raman spectra of G/Cu and G/Ni (i), obtained using photon excitation of 488nm and 532nm respectively.

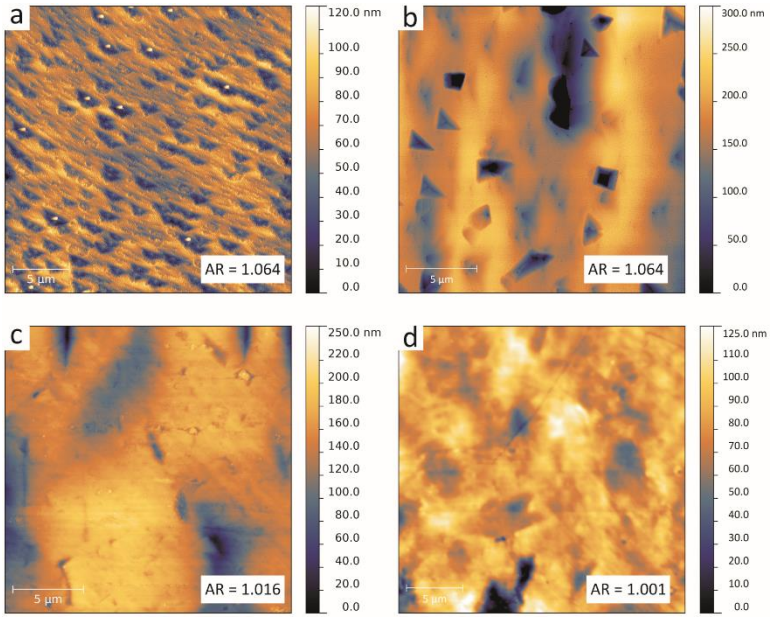

Figure S 2. AFM images of bare Cu (a, b) and Ni (c, d) reference substrate taken at different ambient air exposure time points. The images in (a, c) are taken from samples with t = ~1 week, while those in (b, d) are taken from samples with t = ~1 year.

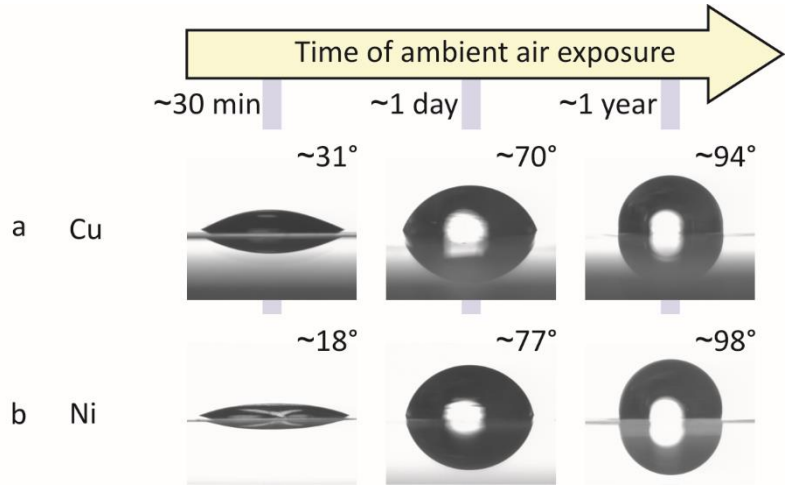

Figure S 3. Contact angle goniometry images of static sessile water drops on the surface of bare Cu (a) and Ni (b) substrates that have been exposed to ambient air for about 30 minutes, 1 day, and 1 year. The ambient air exposure time for these samples is determined from the time at which they were taken out from the reactor right after the heat treatment.

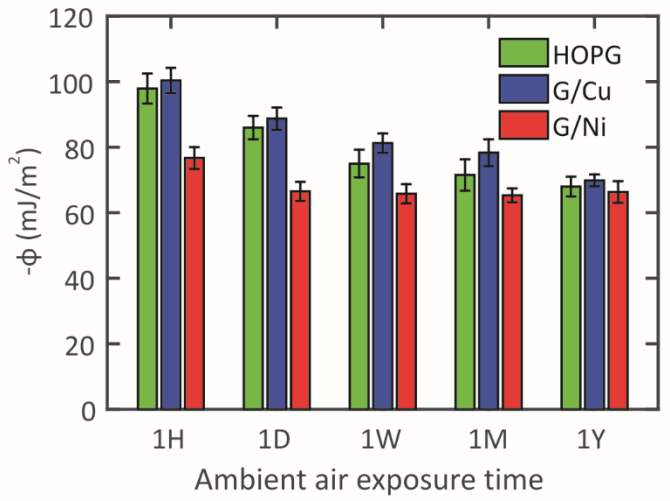

Figure S 4. Interaction potential per unit area (-Φ) between water and supported graphene measured at various ambient air exposure time indicated on the x-axis, i.e. 1 hour (1H), 1 day (1D), 1 week (1W), 1 month (1M), and 1 year (1Y). Φ can be estimated using the modified Young-Dupré equation: $\gamma_L(1 + cos\,\theta) = -\phi$, where γ_L is the surface tension of the water (72.8 mJ m^{-2}).

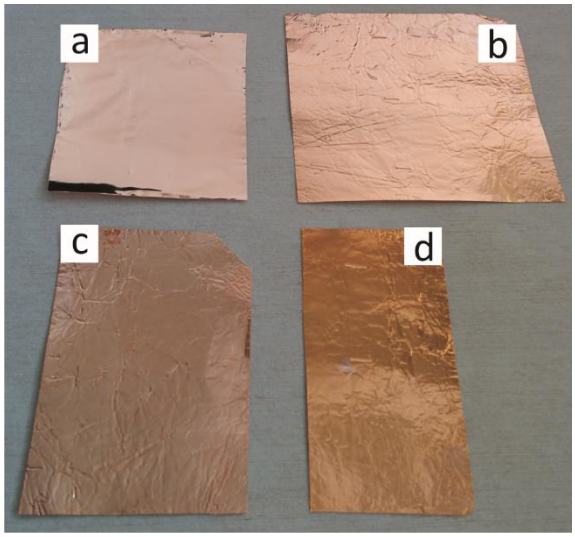

Figure S 5. Optical images of G/Cu and bare Cu taken at different ambient air exposure time points. (a) Image of G/Cu taken immediately after CVD. (b) Image of bare Cu taken immediately after annealing. (c) Image of G/Cu after being exposed to ambient air for about 1 year. (d) Image of bare Cu after being exposed to ambient air for about 1 year. Homogeneous color change from (a) to (c) indicates the oxidation of the underlying Cu substrate. Similarly, homogeneous color change from (b) to (d) indicates the oxidation of the bare Cu. However, the difference in color between (c) and (d) indicates a different oxidation behavior between G/Cu and bare Cu.

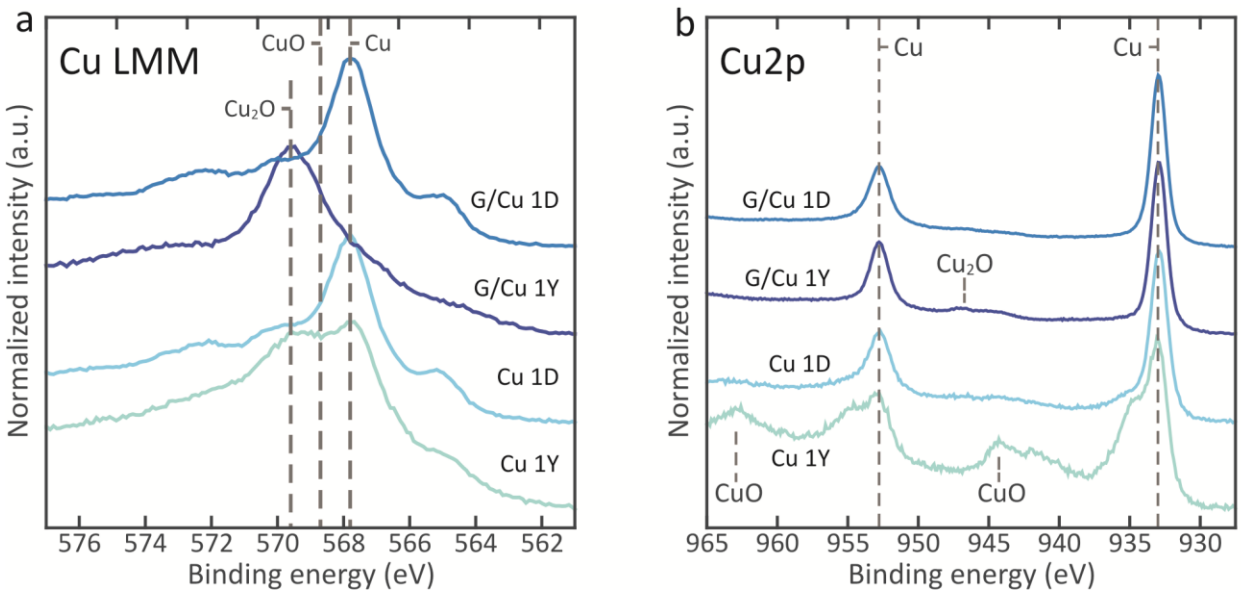

Figure S 6. (a) XPS Cu LMM spectra of G/Cu and bare Cu substrate measured from samples with t = 1 day and t = 1 year. Peaks associated with metallic Cu, CuO, and Cu_2O are found at ~567.8eV, ~568.7eV, and ~569.6eV respectively. (b) XPS Cu2p spectra of G/Cu and bare Cu substrate measured from samples with t = 1 day and t = 1 year. Peaks at ~933eV and ~953eV are associated with metallic Cu ($Cu2p_{3/2}$ and $Cu2p_{1/2}$ core levels respectively), a weak peak at ~947eV is associated with the presence of Cu2O, and peaks at ~944.5eV and ~963eV are associated with the presence of CuO. All spectra are collected with a spectral resolution of ±0.1eV.

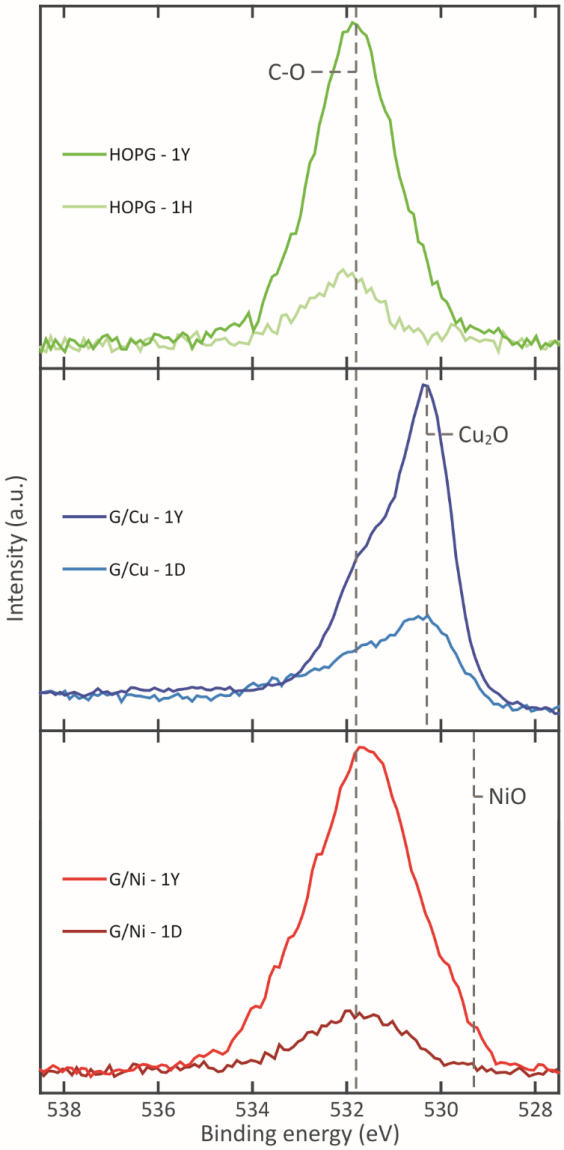

Figure S 7. XPS O1s spectra of HOPG, G/Cu, and G/Ni measured at different ambient air exposure time points. For HOPG, the spectra are measured from samples with t = 1 hour and t = 1 year. For G/Cu and G/Ni, the spectra are measured from samples with t = 1 day and t = 1 year. The peak at ~531.8eV is associated with C-O bonds from adventitious carbon contamination. The O1s spectra of both 1 day old and 1 year old G/Cu are dominated by a peak at ~530.3eV indicating a strong presence of Cu_2O. For 1 day old and 1 year old G/Ni, the lack of a strong

peak at ~529.3eV indicates the absence of NiO. All spectra are collected with a spectral resolution of ±0.1eV.

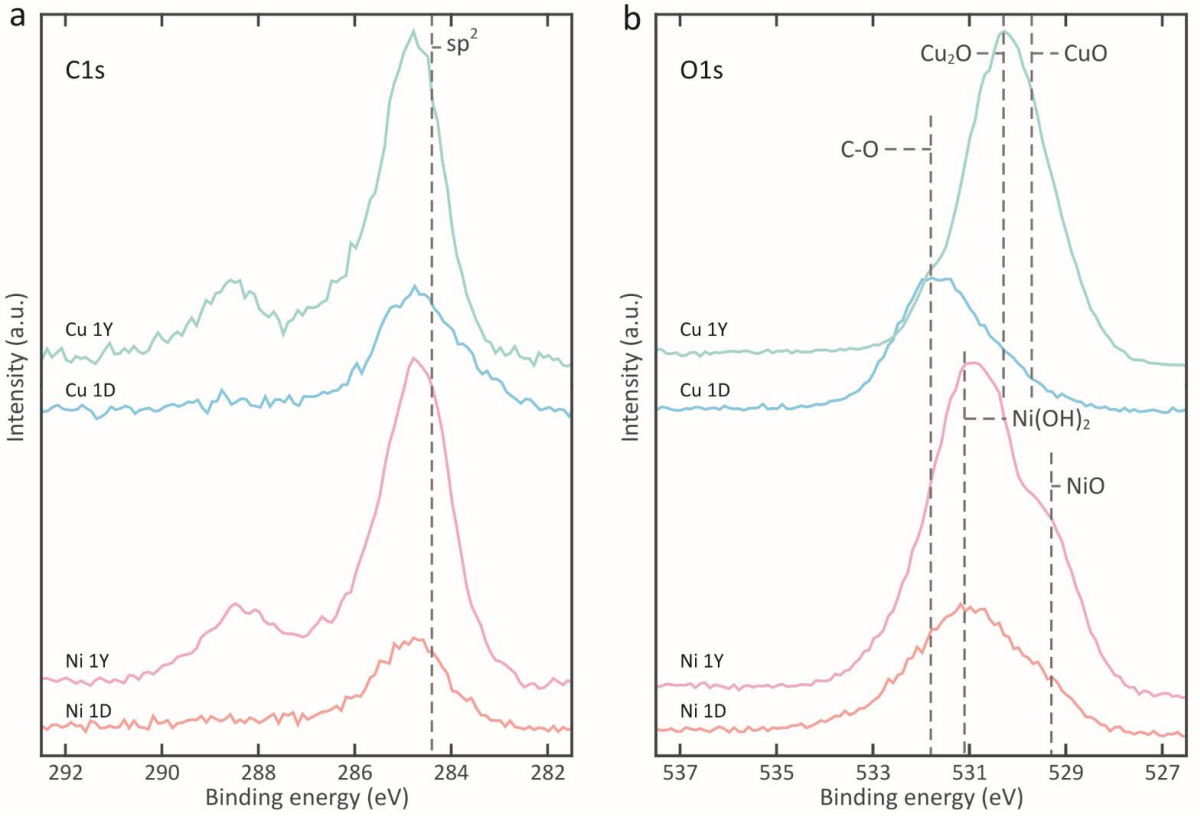

Figure S 8. XPS C1s (a) and O1s (b) spectra of bare Cu and Ni foils with different ambient air exposure time. All spectra are collected from samples with t = 1 day and t = 1 year. In (a), peak associated with sp^2 carbon hybridization is found at ~284.4eV. In (b), the peak at ~531.8eV is associated with C-O bonds from the accumulation of adventitious carbon contamination. The O1s spectrum of 1 year old G/Cu is dominated by peaks at ~530.3eV and ~529.7eV, indicating a strong presence of both Cu_2O and CuO. The O1s spectrum of 1 year old G/Ni is dominated by a peak at ~531.1eV and a shoulder at ~529.3eV, indicating a strong presence of $Ni(OH)_2$ and NiO. All spectra are collected with a spectral resolution of ±0.1eV.

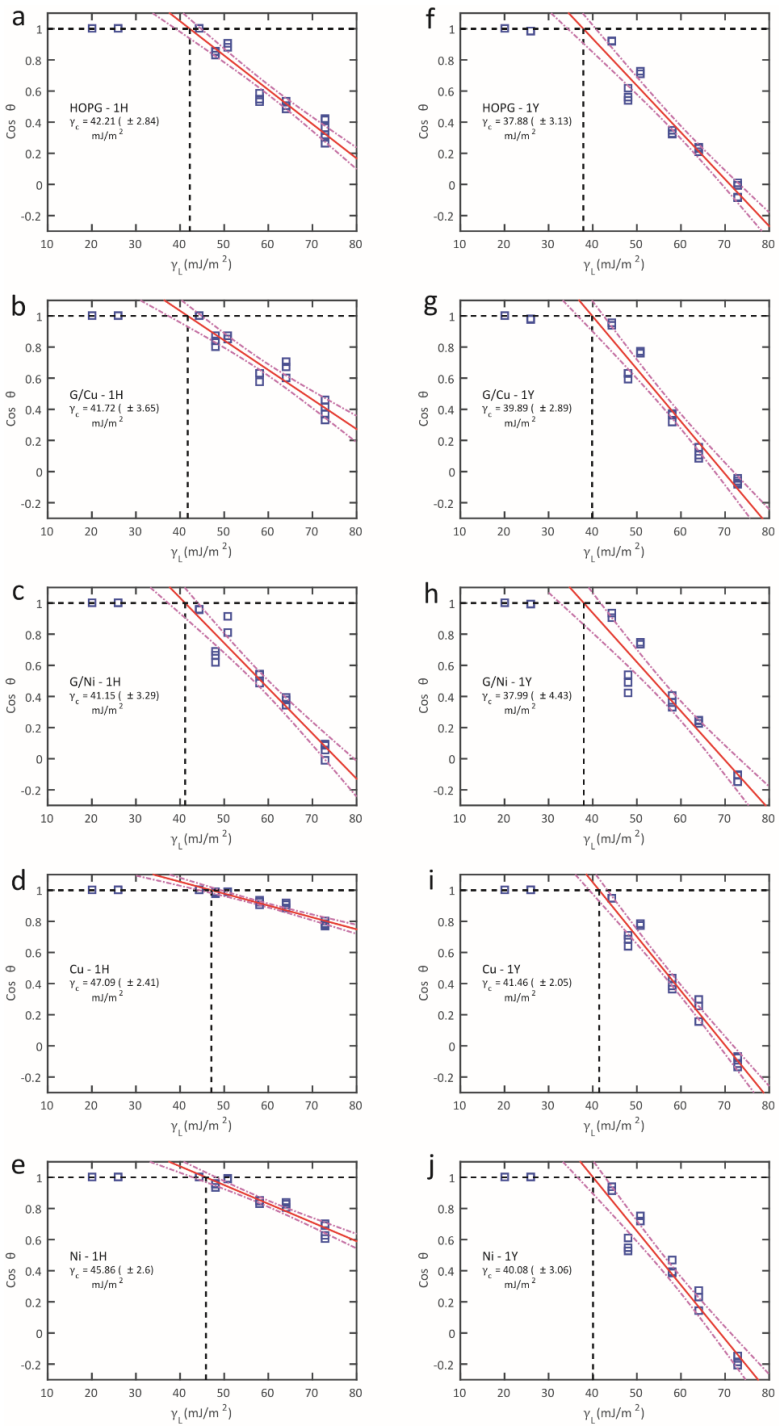

Figure S 9. Determination of critical surface tension (γ_C) of graphene and bare metal samples according to the Zisman model at different ambient air exposure time, i.e. 1 hour for samples (a–e), and 1 year for samples (f–j). The solid line indicates the regression line of the data using ordinary least square method, and the dotted lines indicate 95% prediction interval.

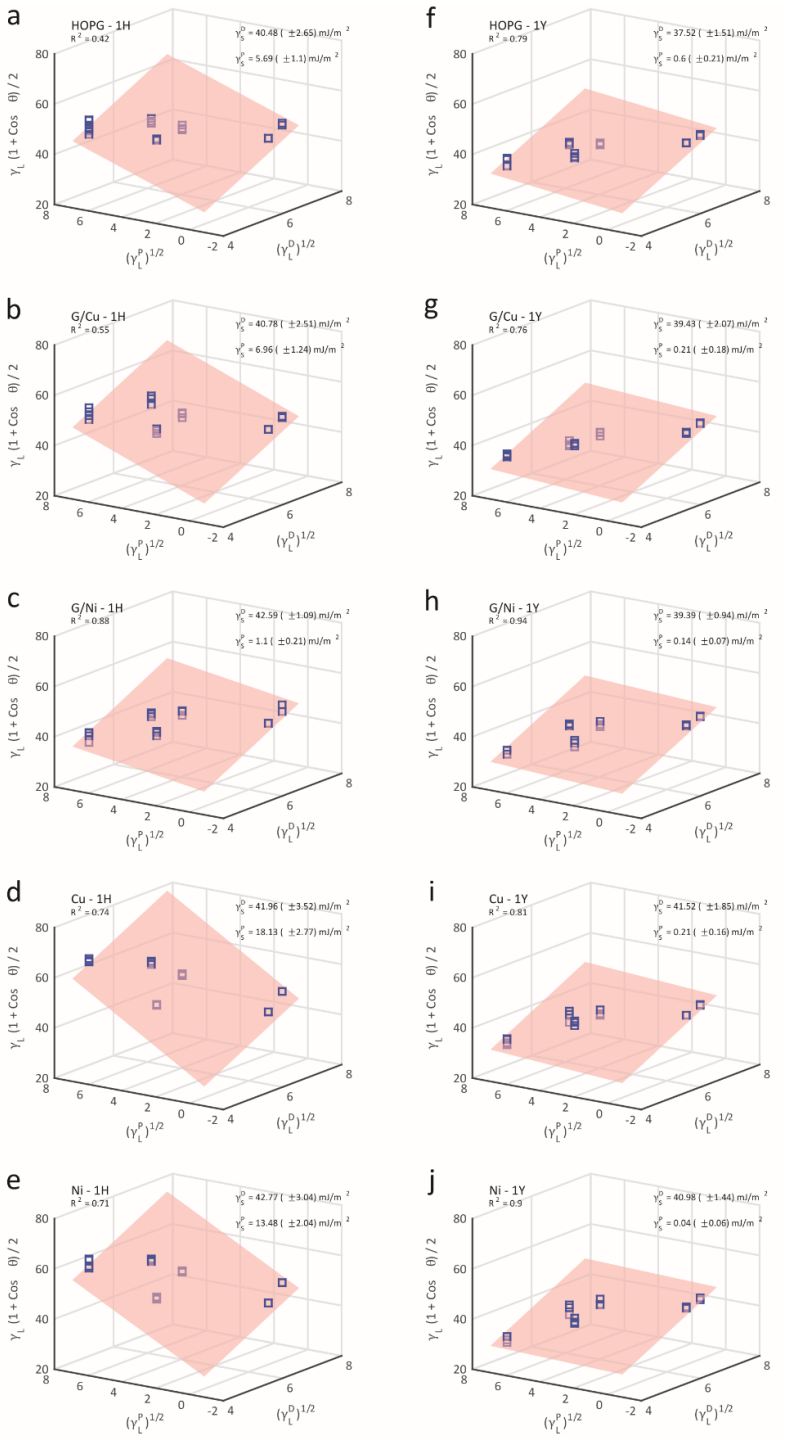

Figure S 10. Determination of surface free energy (γ_S) of graphene and bare metal samples according to the Owens–Wendt (extended Fowkes) model at different ambient air exposure time, i.e. 1 hour for samples (a–e), and 1 year for samples (f–j). The translucent plane indicates the regression plane of the data using ordinary least square method.

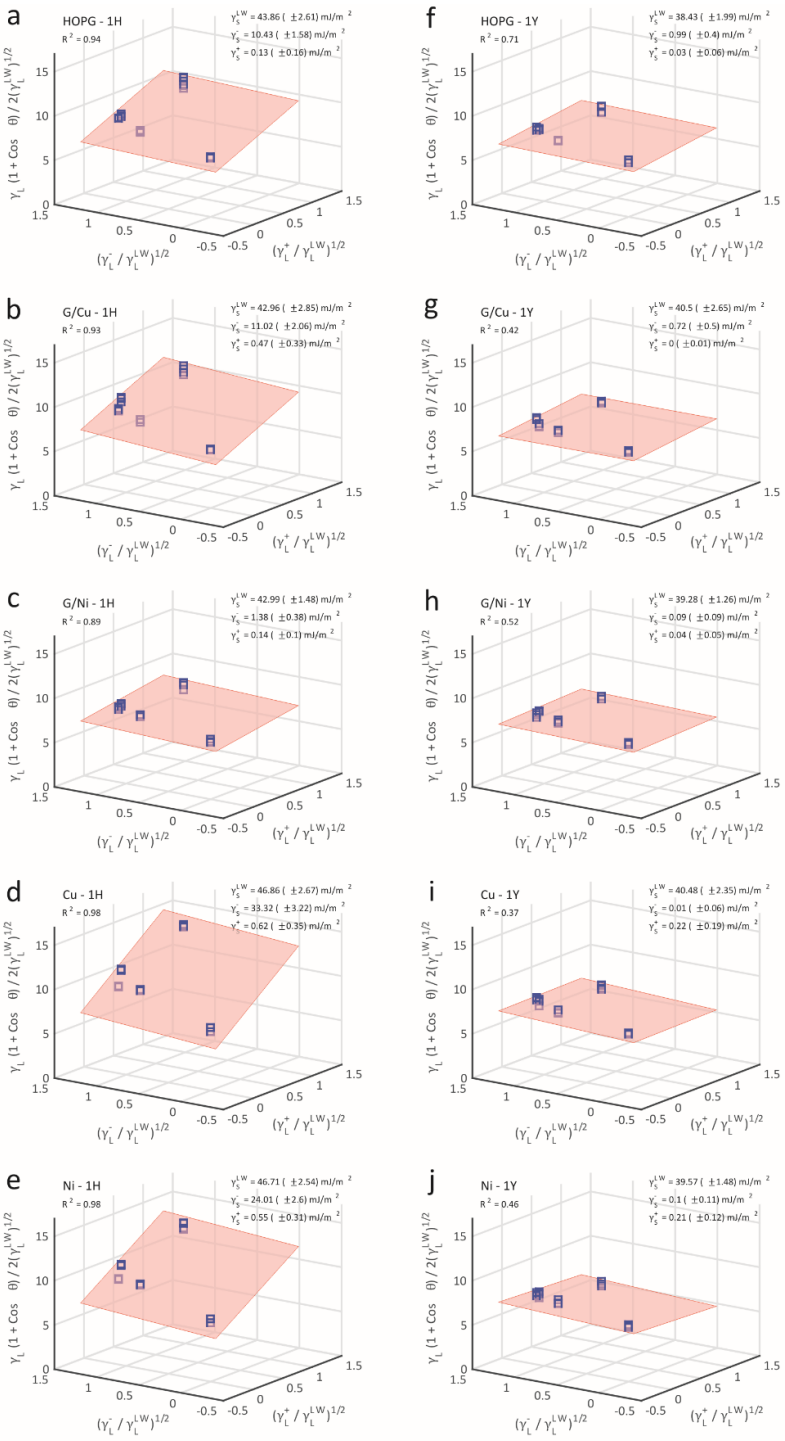

Figure S 11. Determination of surface free energy (γ_S) of graphene and bare metal samples according to the van Oss–Chaudhury–Good model at different ambient air exposure time, i.e. 1 hour for samples (a–e), and 1 year for samples (f–j). The translucent plane indicates the regression plane of the data using ordinary least square method.

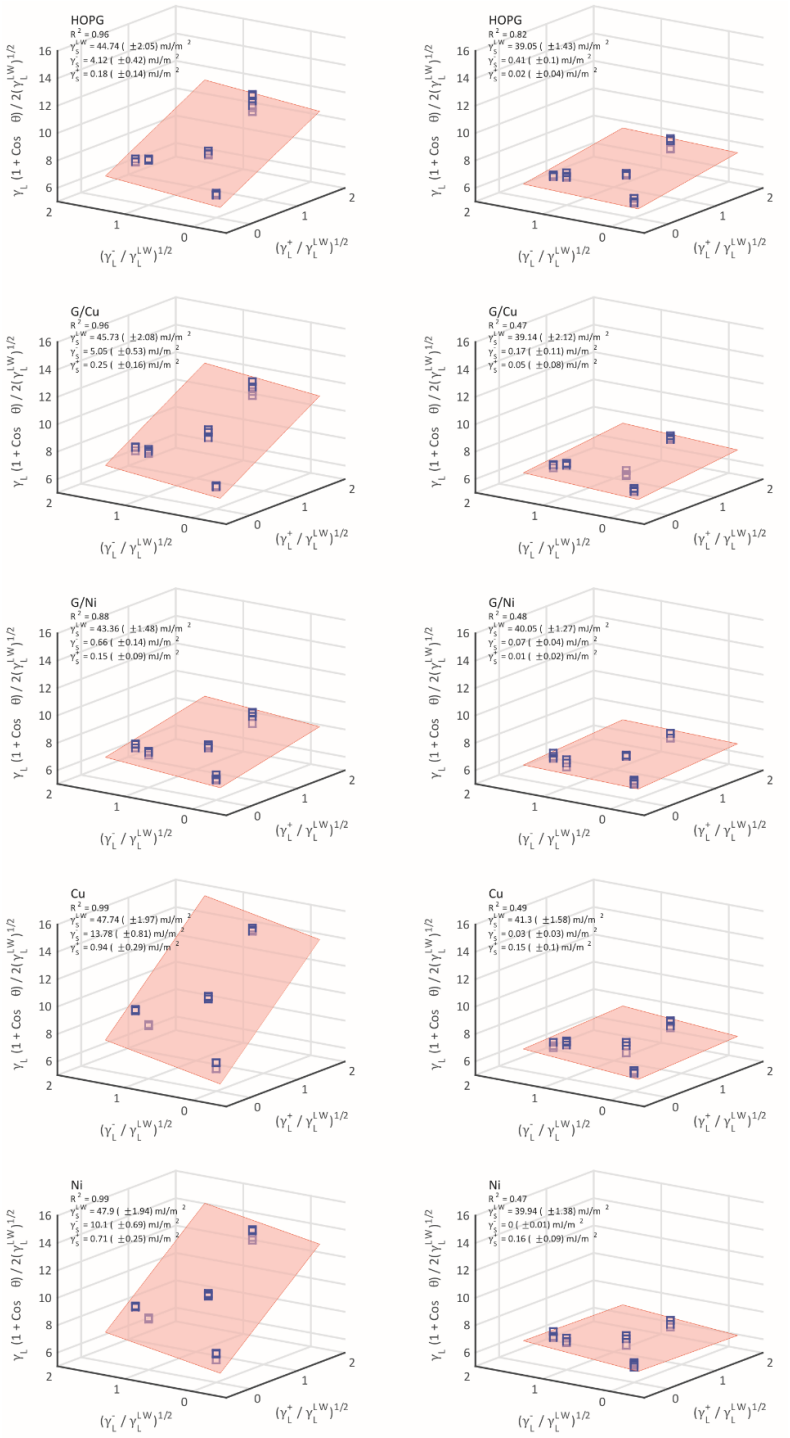

Figure S 12. Determination of surface free energy (γ_S) of graphene and bare metal samples according to the adjusted van Oss–Chaudhury–Good model at different ambient air exposure time, i.e. 1 hour for samples (a–e), and 1 year for samples (f–j). The translucent plane indicates the regression plane of the data using ordinary least square method.

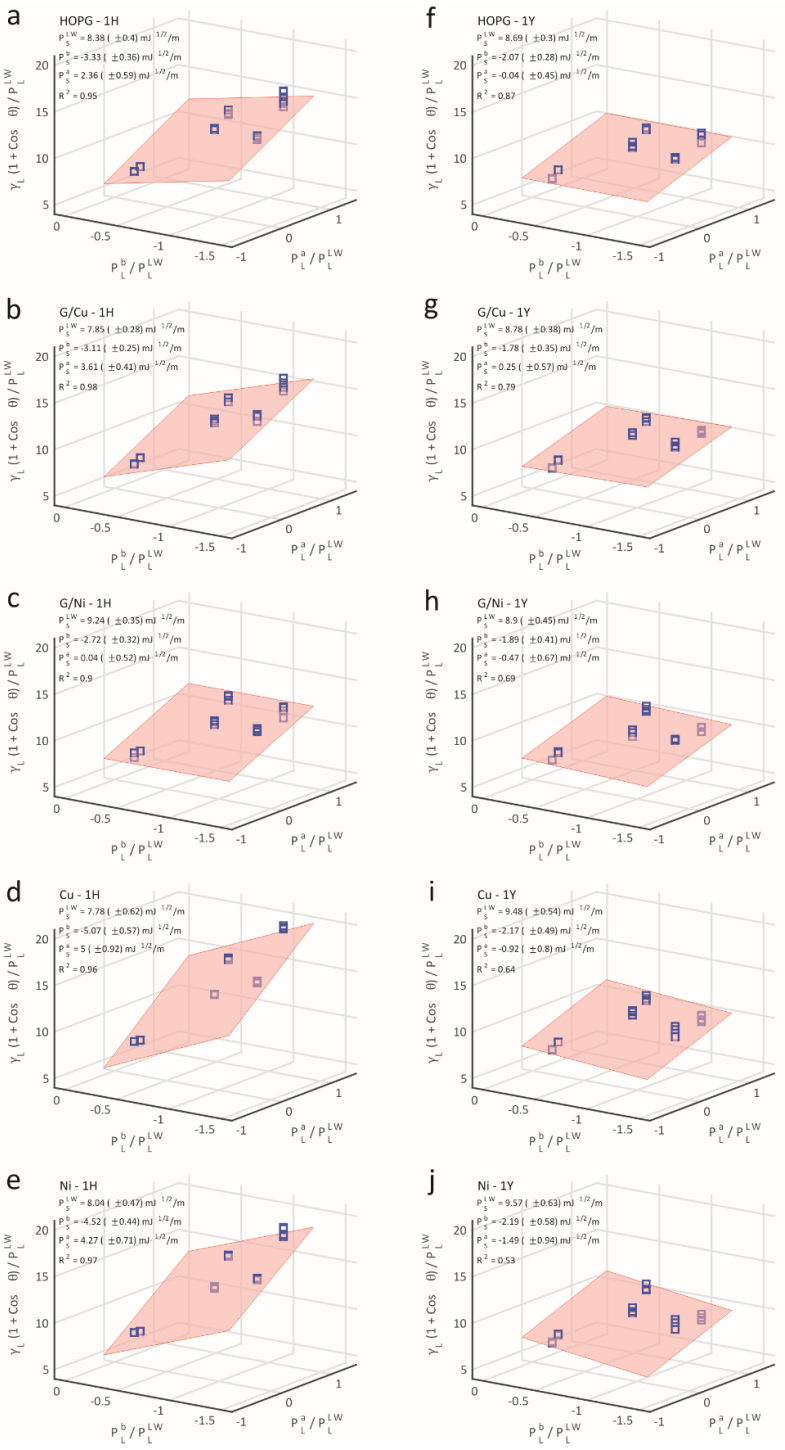

Figure S 13. Determination of surface free energy (γ_S) of graphene and bare metal samples according to the Chang–Chen model at different ambient air exposure time, i.e. 1 hour for samples (a–e), and 1 year for samples (f–j). The translucent plane indicates the regression plane of the data using ordinary least square method.

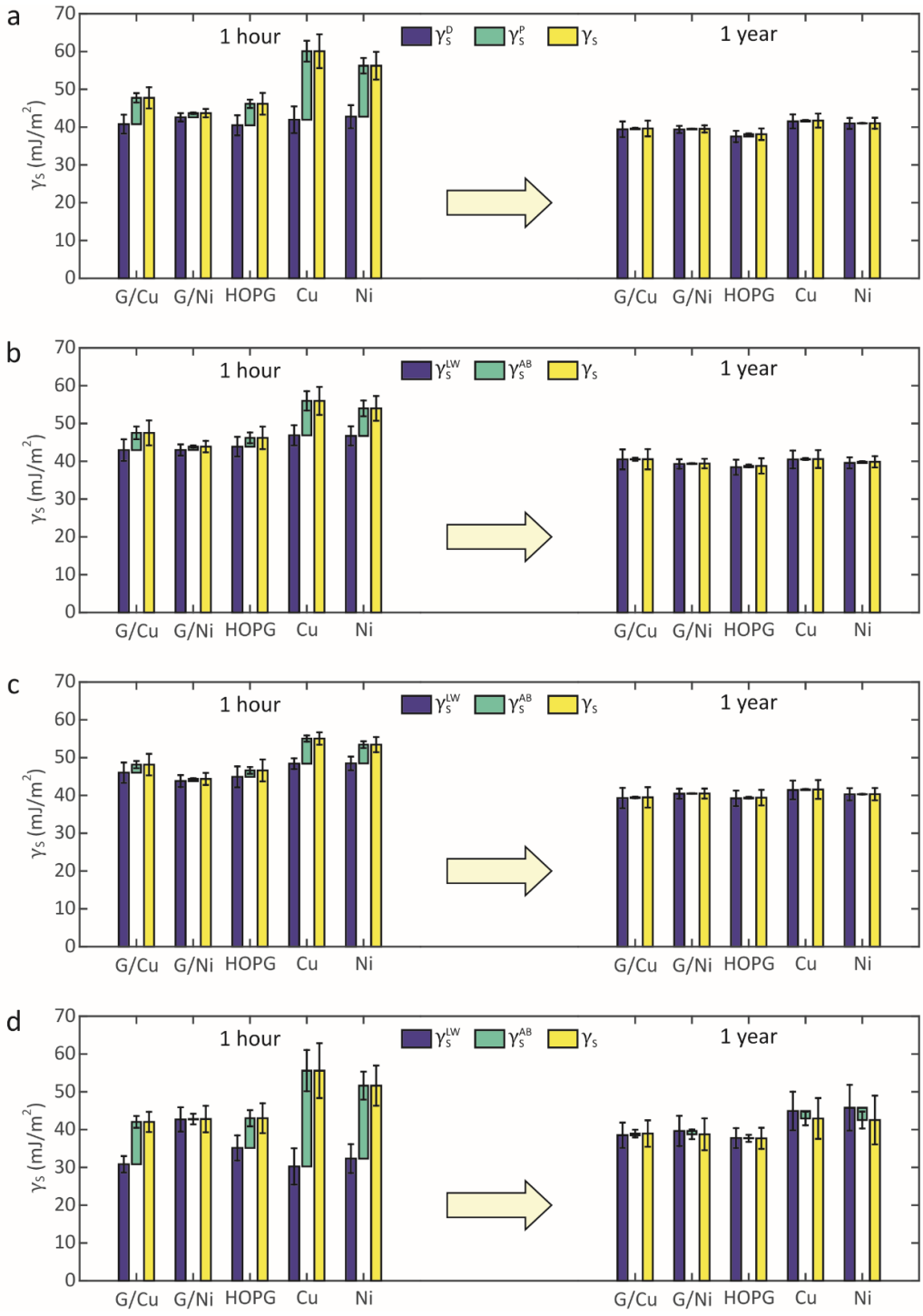

Figure S 14. The evolution of surface free energy (γ_S), along with its Lifshitz-van der Waals (γ_S^{LW}) and Lewis acid-base (γ_S^{AB}) components, of supported graphene, HOPG, and bare metal samples based on calculations using the Owens–Wendt (a), van Oss–Chaudhury–Good (b), adjusted van Oss–Chaudhury–Good (c), and Chang–Chen (d) models obtained from two

different sets of samples, each had been exposed to ambient air for either 1 hour or 1 year. All error bars indicate the standard error of regression.

REFERENCES

(1) Quéré, D. Rough Ideas on Wetting. *Phys. A Stat. Mech. its Appl.* **2002**, *313* (1-2), 32–46.

(2) Swain, P. S.; Lipowsky, R. Contact Angles on Heterogeneous Surfaces: A New Look at Cassie's and Wenzel's Laws. *Langmuir* **1998**, *14* (23), 6772–6780.

(3) Raj, R.; Maroo, S. C.; Wang, E. N. Wettability of Graphene. *Nano Lett.* **2013**, *13* (4), 1509–1515.

(4) Rafiee, J.; Mi, X.; Gullapalli, H.; Thomas, A. V; Yavari, F.; Shi, Y.; Ajayan, P. M.; Koratkar, N. A. Wetting Transparency of Graphene. *Nat. Mater.* **2012**, *11* (3), 217–222.

(5) Schrader, M. E. Young-Dupre Revisited. *Langmuir* **1995**, *11* (9), 3585–3589.

(6) Li, Z.; Wang, Y.; Kozbial, A.; Shenoy, G.; Zhou, F.; McGinley, R.; Ireland, P.; Morganstein, B.; Kunkel, A.; Surwade, S. P.; et al. Effect of Airborne Contaminants on the Wettability of Supported Graphene and Graphite. *Nat. Mater.* **2013**, *12* (10), 925–931.

(7) Shih, C.-J.; Wang, Q. H.; Lin, S.; Park, K.-C.; Jin, Z.; Strano, M. S.; Blankschtein, D. Breakdown in the Wetting Transparency of Graphene. *Phys. Rev. Lett.* **2012**, *109* (17), 176101.

(8) Etzler, F. M. Determination of the Surface Free Energy of Solids. *Rev. Adhes. Adhes.* **2013**, *1* (1), 3–45.

(9) Zisman, W. A. Relation of Equlibrium Contact Angle to Liquid and Solid Constitution. In *Contact Angle, Wettability, and Adhesion*; Fowkes, F. M., Ed.; Advances in Chemistry; American Chemical Society: Washington, D.C., 1964; Vol. 43, pp 1–51.

(10) Owens, D. K.; Wendt, R. C. Estimation of the Surface Free Energy of Polymers. *J. Appl. Polym. Sci.* **1969**, *13* (8), 1741–1747.

(11) Van Oss, C. J.; Chaudhury, M. K.; Good, R. J. Interfacial Lifshitz-van Der Waals and Polar Interactions in Macroscopic Systems. *Chem. Rev.* **1988**, *88* (6), 927–941.

(12) Volpe, C. D.; Siboni, S. Some Reflections on Acid–Base Solid Surface Free Energy Theories. *J. Colloid Interface Sci.* **1997**, *195* (1), 121–136.

(13) Chang, W. V.; Qin, X. Repulsive Acid - Base Interactions: Fantasy or Reality? In *Acid-base Interactions: Relevance to Adhesion Science and Technology*; Mittal, K. L., Ed.; VSP: Utrecht, The Netherlands, 2000; pp 3–54.

(14) Chen, F.; Chang, W. V. Applicability Study of a New Acid Base Interaction Model in Polypeptides and Polyamides. *Langmuir* **1991**, *7* (10), 2401–2404.

(15) Kozbial, A.; Li, Z.; Conaway, C.; McGinley, R.; Dhingra, S.; Vahdat, V.; Zhou, F.; D'Urso, B.; Liu, H.; Li, L. Study on the Surface Energy of Graphene by Contact Angle Measurements. *Langmuir* **2014**, *30* (28), 8598–8606.